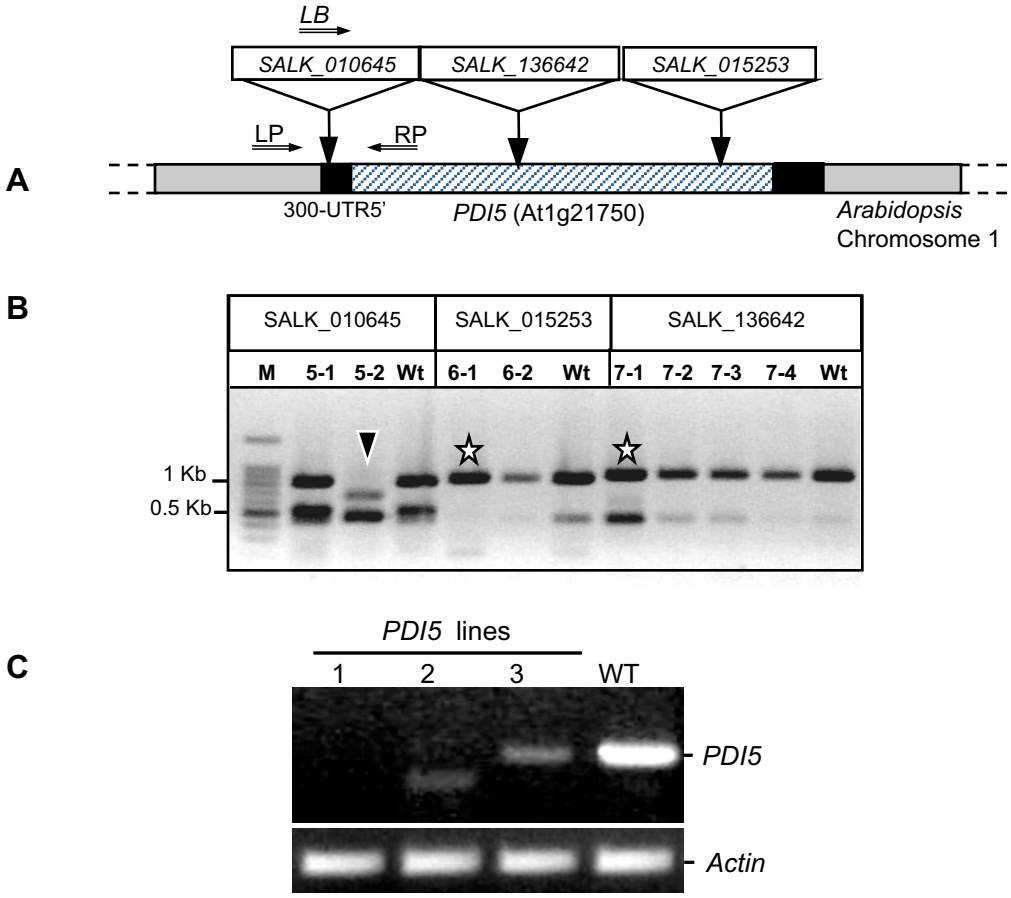

Supplemental Figure 1. Genetic Map of *Arabidopsis PDI5* Gene and T-DNA Insertion Mutant Lines.

(A) Schematic representation of the *PDI5* gene (locus no. AAD41430) and the three locations of T-DNA SALK_Insertions on *Arabidopsis* chromosome 1. The T-DNA SALK_010645 insertion site is located between nucleotides 76455543 and 7645718; T-DNA SALK_136642 and SALK_015253 are located between nucleotides 7646531 and 7646635, and 7647678 and 7648117 respectively.

(B) PCR-amplified genomic DNA extracted from wild-type and *PDI5Δ* mutant plants. To confirm that the PDI5 mutation is linked to the T-DNA SALK insertion, a pool of plants, each containing DNA from the three mutant lines, were prepared and checked by PCR analysis for the specific amplification of the T-DNA left border (LB) product and absence of the amplification in the wild-type plant. PCR analysis of DNA from *pdi5Δ* SALK_010645 plants 5-1, 5-2, WT (two different plants from the #5 pool of Salk_010645 and a wild type). Plant 5-2 reveals one band of approximately 0.5 Kbp (pointed to by the arrow), which confirms that the plant is the homozygous mutant for T-DNA insertion in *pdi5Δ* and lack the wild-type band (1.0 Kbp). Plant 5-1 is a heterozygote or wild type. 6-1, 6-2, WT (two different plants from the #6 pool of Salk_015253 and a wild type). The 6's appear to be all heterozygotes. 7-1, 7-2, 7-3, 7-4, WT (four different plants from the #7 pool of Salk_136642 and a wild type). The 7's appear to be all heterozygotes. Stars show the wild-type 1.0 Kbp band produced by the LB and RP primers in the heterozygous lines SALK_136642 and SALK_015253.

(C) RT-PCR analysis of the three *PDI5* gene insertion lines and wild type. Lane 1 (Salk_010645), gave no detectable mRNA, which confirms the immunoblot result (Fig. 2). RT-PCR in lane 2 (Salk_015253) gives a smaller band suggesting cryptic transcription yielding a truncated mRNA. Lane 3 (Salk_136642) yields a full-length mRNA. The insertion line represented in lane 3, the T-DNA insertion resides in intron (Figure 1A) of the *PDI5* gene. Since the lines in lanes 2 and 3 show some expression, the Salk_010645 line was used in this work. The RT-PCR products are representative of two independent experiments done in duplicate. The intense larger band in the wild type lane indicates high expression of full length *PDI5 mRNA.*

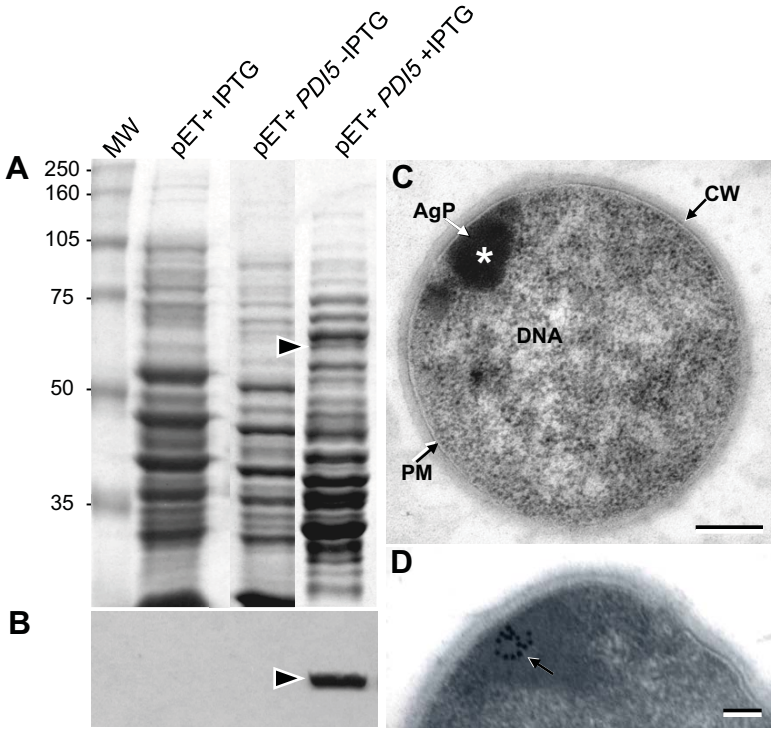

Supplemental Figure 2. Expression and Immunodetection of Recombinant PDI5 Protein in *E. coli* Cells.

A polyclonal rabbit antibody was generated against the PDI5-specific peptide DKNKDTVGEPK (amino acid residues 478-488 bold italic underlined in Figure 1C). A full 1506-bp *PDI5* cDNA (locus no AAD41430) fragment encoding the polypeptide PDI5 was cloned and expressed E. *coli*. The specificity of the antibodies was tested in situ by immunogold labeling of high-pressure frozen *E, coli* cells expressing the PDI5 recombinant protein as well as in western blots of protein extracts of these cells.

(A) Coomassie brilliant blue staining of PDI5 expressed in E. *coli*. Lane 1, standard molecular weight (MW). Lane 2, empty pET-25b(+) vector with IPTG. Lane 3 pET-25b(+) plus *PDI5* cDNA without IPTG induction. Lane 4 PDI5 expression in pET vector plus *PDI5* cDNA with IPTG induction. The arrow points to the recombinant PDI5 protein expressed in *E. coli* at 68-70 kDa that is recognized by the polyclonal anti-PDI5 antibodies in the western blot, and indicated with an arrow in **(B)**. **(C)** and **(D)** Thin section electron micrographs of *E. coli* cells expressing pET-25b(+) vector plus *PDI5* cDNA with IPTG induction. The anti-PDI5 antibody labels the darkly stained aggregate of recombinant PDI5 protein in **(D)** indicating the specificity of the antiserum to the peptide. AgP, protein aggregate; CW, cell wall; PM, plasma membrane. Bars: **(C)** and **(D)** = 0.3 μm.

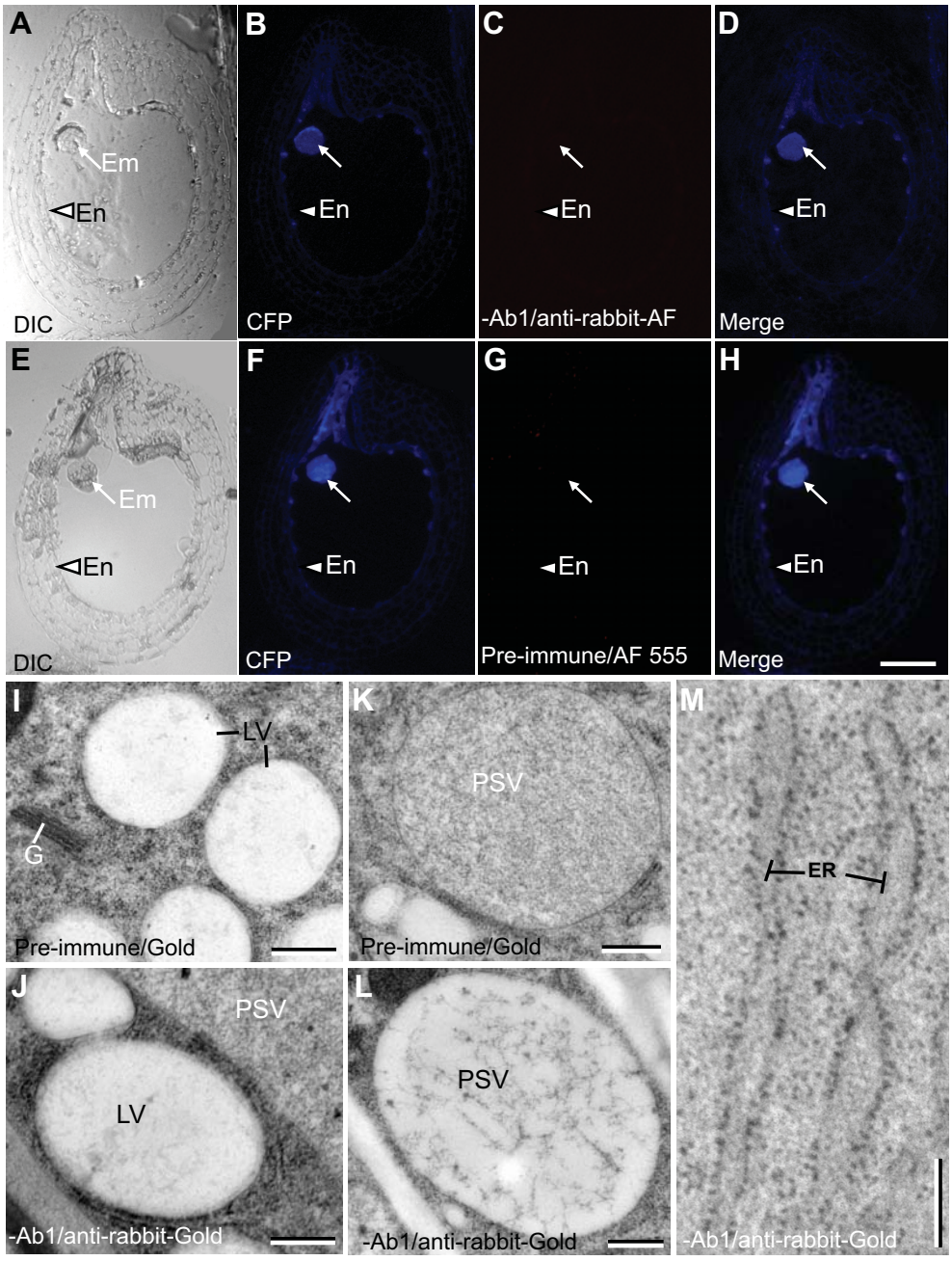

Supplemental Figure 3. Immunological Controls of PDI5 Antibody Specificity in the Endothelial Cells Layer and in Endothelial Cells.

(A) to **(D)** Immunofluorescence labeling control using anti-rabbit IgG secondary antibody tagged Alexa-Fluor 555 (AF 555) with omission of the primary antibody (-Ab1). **(A)** Differential interference contrast (DIC) micrographs of a developing seed. White arrowheads mark the maternal tissue endothelial cell layer (En) and white arrows point to the embryo (Em) at the globular stage of development. **(B)** Auto-fluorescence micrograph of developing seed labeled with AF 555 and viewed using a CFP filter set. **(C)** Immunofluorescence image of a developing seed labeled with a secondary antibody anti-rabbit IgG tagged Alexa-Fluor 555. **(D)** Merged image DIC/CFP/AF 555. **(E)** to **(H)** Immunofluorescence labeling micrographs of developing seed labeled with a substituted pre-immune rabbit serum as a primary antibody and anti-rabbit IgG tagged Alexa-Fluor 555 as a secondary antibody. **(E)** Differential interference contrast. **(F)** Auto-fluorescence image viewed under CFP filter set. **(G)** Alexa-Fluor 555 immunofluorescence wavelength. **(H)** Merged image DIC/CFP/AF 555.

(I) to **(M)** Immunogold labeling control experiment performed without the primary antibodies including anti-PDI5, anti-δ-TIP, anti-RD21 and anti-2S. **(I)** Lytic vacuoles (LVs) labeled with pre-immune serum. **(J)** LVs labeled with anti-rabbit IgG tagged gold particle without the primary antibodies. **(K)** Protein storage vacuole (PSV) labeled with pre-immune serum as a primary antibody. **(K)** PSV labeled with secondary antibody anti-rabbit IgG tagged gold particles without a primary antibody (-Ab1). **(M)** ER control labeled with a secondary antibody anti-rabbit IgG. In all no gold particles are observed in the LVs, PSVs nor ER. These controls confirm the specificity of the primary and secondary antibodies over the endothelial cells layer and the endothelial cell organelles. Bars: **(H)** = 100 μm also applies to images **(A)** to **(G)**; **(I), (K)** and **(L)** = 0.40 μm; **(J)** = 0.30 μm and **(M)** = 0.20 μm.

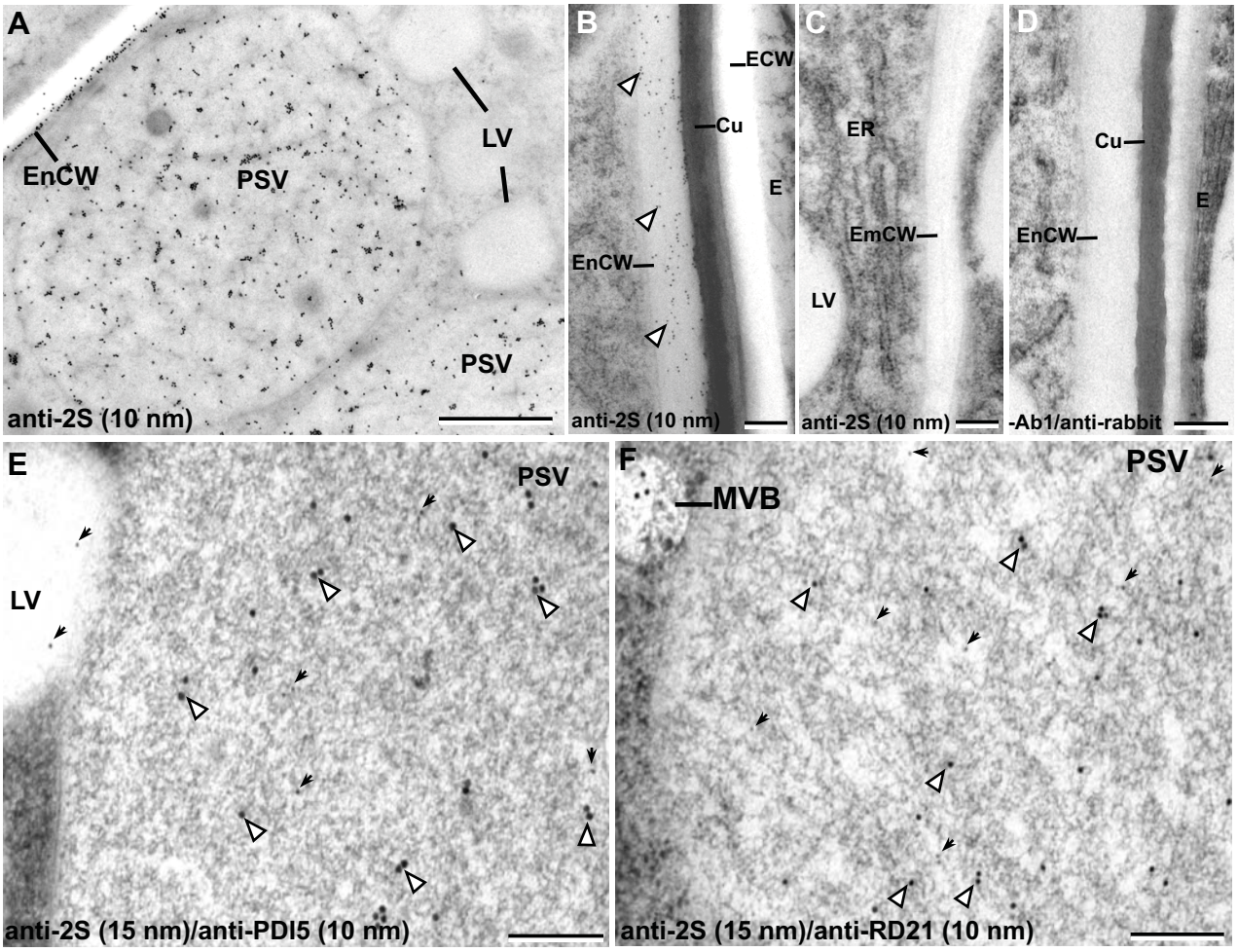

Supplemental Figure 4. Single- and Double-Immunogold Labeling of PSVs in Endothelial Cells with anti-2S Albumin with/without anti-PDI5 or anti-RD21 Antibodies.

To support the findings of the co-immunolocalization of anti-PDI5 with anti-RD21 antibodies, we performed the controls by co-immunolocalizing anti-PDI5 or anti-RD21 with an anti-storage protein antibody, anti-2S albumin over the protein storage vacuoles (PSVs). **(A)** Immunolocalization of storage protein 2S albumin to the PSVs and to the cell wall of endothelial cells. Anti-2S albumin antibody labeled over the PSV, and was seen over the endothelial cell wall (EnCW, (**A** and **B**)), and in the multivesicular body (MVB, in **(F)**). Anti-2S albumin gold particles were not seen in the lytic vacuoles (LVs, **A**, **C** and **E**) in the embryonic cell wall (EmCW, (**C**)) or in the endosperm (E) cell wall (ECW, (**B**)) facing the cuticular layer (Cu). Control experiments with omission of the primary antibody anti-2S showed no labeling of the endothelial cell walls **(D)**. Controls in which the anti-2S was omitted or substituted with pre-immune rabbit serum showed no labeling of PSVs and LVs (Supplemental Figure 3, **I**, **J, K** and **L**).

(E) Co-Immunolocalization of anti-2S and anti-PDI5 to the PSV. (**F**) Co-immunolocalization of anti-2S and anti-RD21 to the PSV. We demonstrated that PDI5 or cysteine protease RD21 (black arrowheads) do not co-localize with protein storage anti-2S antibody (white arrowheads) over PSVs within the senescing endothelial cells. Bars: **(A)** = 1 μm; **(B), (C)** and **(D)** = 0.20 μm; **(E)** = 0.40 μm and **(F)** = 0.35 μm.

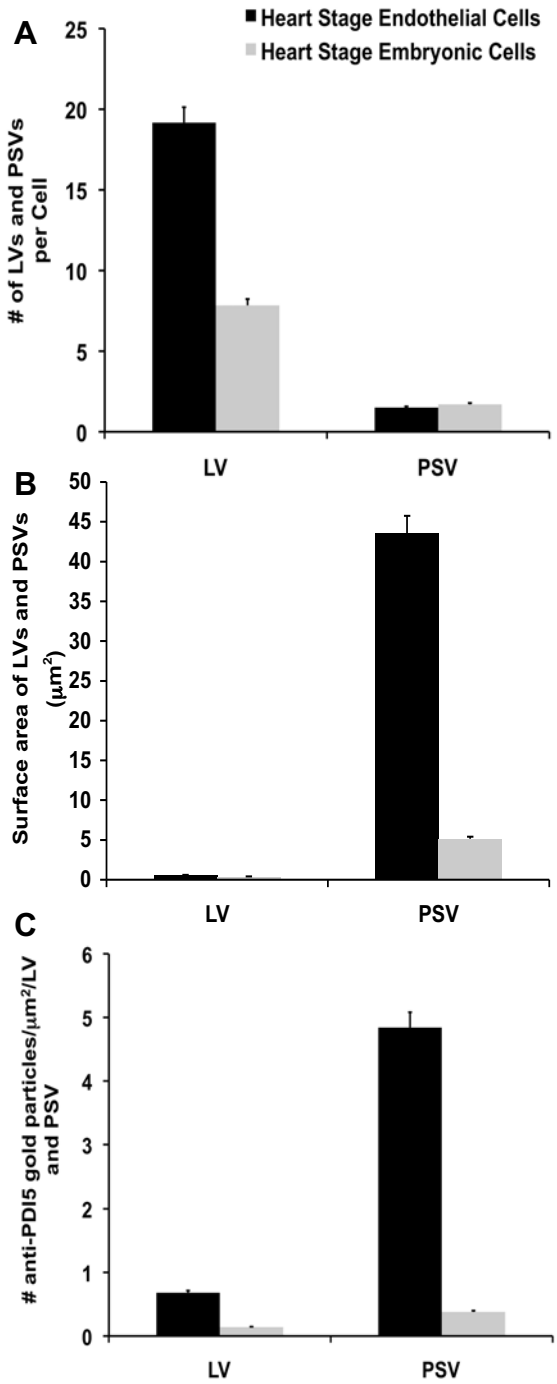

Supplemental Figure 5. Quantitative, Comparative Analysis of the Number and Cross Sectional Area of LV and PSV, and of anti-PDI5 Labeling in Senescing Heart Stage Endothelial and Embryonic Cells.

(A) Number of lytic vacuoles (LVs) and protein storage vacuoles (PSVs) per endothelial and embryonic cell. **(B)** Cross sectional area (μm^2) of lytic and protein storage vacuoles per endothelial and embryonic cell. **(C)** Number of anti-PDI5 gold particles per lytic and per protein storage vacuole in endothelial and embryonic cells. Although the number of LVs is greater than the number of PSVs in heart stage endothelial cells (LVs/PSVs number ratio is ~2.5). The cross sectional area (μm^2) of PSVs is ~ 40 times greater than the LVs. In embryonic cells, both the numbers and cross sectional areas of the vacuoles are smaller than in endothelial cells. The levels of anti-PDI5 labeling over endothelial cell vacuoles (LVs and PSVs), was also considerably higher than over the vacuoles of embryonic cells (C). In turn the number of gold labels over PSVs was ~ 5 fold higher over the PSVs. These findings suggest that PDI5 is more highly expressed in heart stage endothelial than in embryonic cells, and that within the former the bulk of the PDI5 accumulates in PSVs. The PSV/LV labeling ratio is ~7.2 in both cell types.

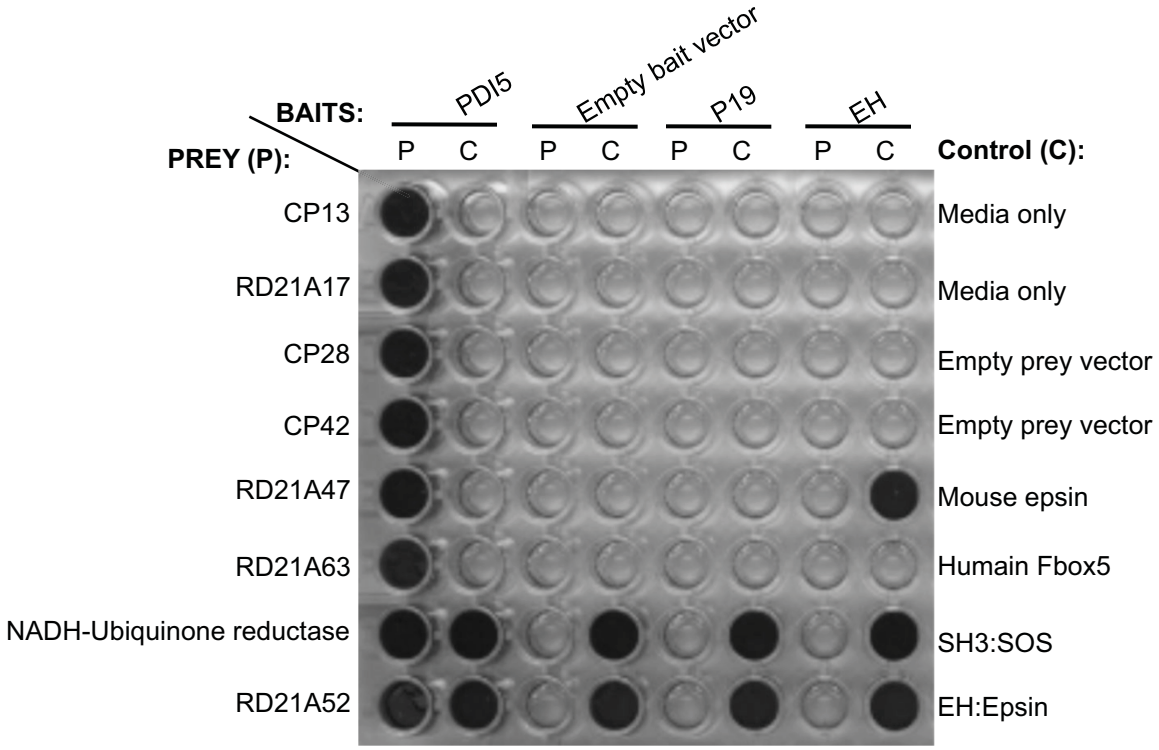

Supplemental Figure 6. Interaction of PDI5 with Selected Prey in Yeast Two-Hybrid Assay.

A ß-galactosidase assay demonstrates interaction between prey (columns labeled 'P' and listed in left-hand column: *Arabidopsis* cysteine proteinase / thiol protease, putative (CP), *Arabidopsis* cysteine proteinase / thiol protease (RD21A), and *Arabidopsis* NADH-Ubiquinone reductase) isolated in the yeast two-hybrid screen with *Arabidopsis* PDI5 as bait. Baits include PDI5, the empty bait vector (pBUTE) and the following inserts cloned in-frame with the GAL4 DNA binding domain: the human SKP1 homologue (P19) and the EF-hand domain of intersectin (EF). Wells in the control lane (columns labeled 'C') include media only, empty prey (activation domain) vector (pGAD-C1), prey construct expressing mouse epsin, prey construct expressing human Fbox5 and two pre-mated interacting pairs: SH3:SOS and EH:Epsin. ß-gal activity was assayed in cultures expressing the bait and prey following mating and selection in interaction selection media (histidine dropout plus 1 mM 3AT). Image was scanned following overnight incubation at 37^{o}C.

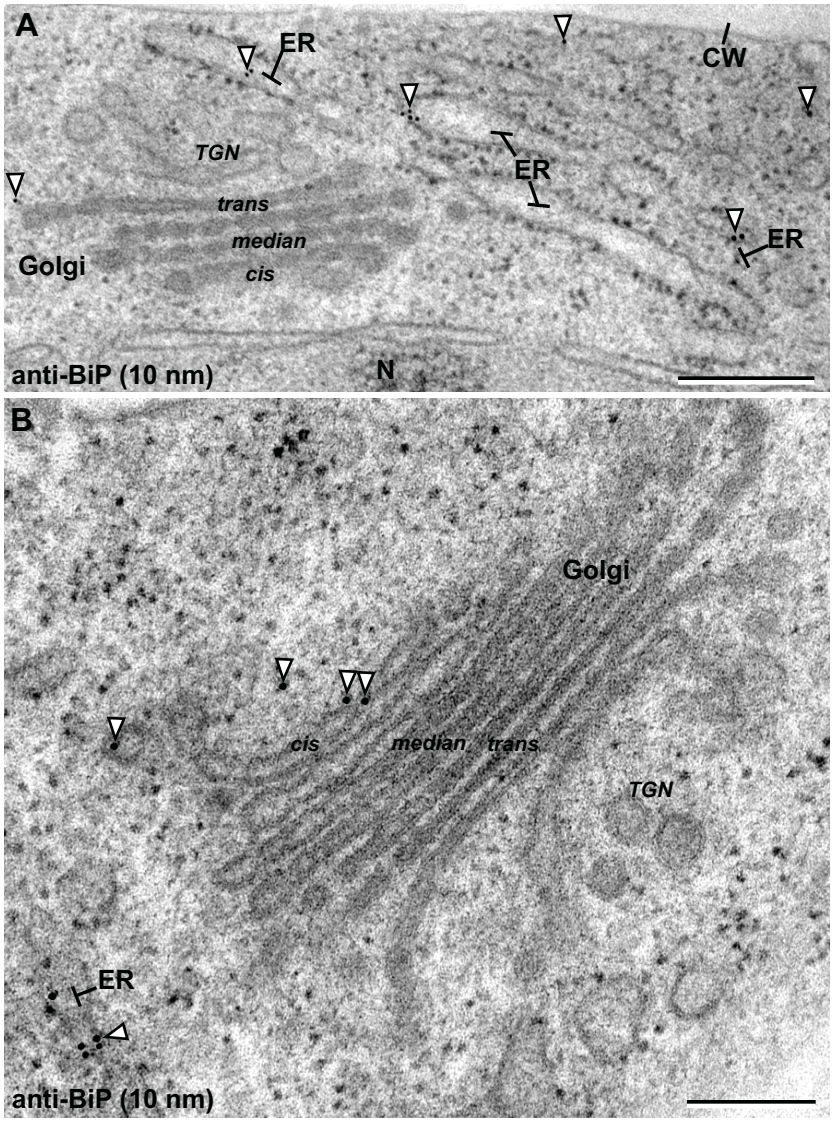

Supplemental Figure 7. Immunogold Labeling of BiP (Binding Protein) in Endothelial Cells.

(A) and **(B)** Polyclonal anti-BiP antibodies (10 nm of gold particles, open arrows) immunolabeled thin section micrographs illustrating the distribution of BiP in ER and Golgi cisternae. Most of the labeling is over ER cisternae, and some labeling is over cis-Golgi cisternae and small vesicles between the ER and Golgi cisternae. Quantitation of labeling in 9 thin section micrographs: ER: 78 gold particles (81%), cis-Golgi cisternae: 15 gold particles (16%); median/trans/TGN cisternae: 3 gold particles (3%). CW, cell wall; N, nucleus. Bars: **(A)** = 0.30 μm and **(B)** = 0.20 μm.